

Mirror Descent Search and its Acceleration[☆]

Megumi Miyashita^a, Shiro Yano^b, Toshiyuki Kondo^b

^a*Dept. of Computer and Information Sciences, Graduate School of Engineering,
Tokyo University of Agriculture and Technology, Tokyo, Japan*

^b*Division of Advanced Information Technology and Computer Science, Institute of Engineering,
Tokyo University of Agriculture and Technology, Tokyo, Japan*

Abstract

In recent years, attention has been focused on the relationship between black-box optimization problem and reinforcement learning problem. In this research, we propose the Mirror Descent Search (MDS) algorithm which is applicable both for black box optimization problems and reinforcement learning problems. Our method is based on the mirror descent method, which is a general optimization algorithm. The contribution of this research is roughly twofold. We propose two essential algorithms, called MDS and Accelerated Mirror Descent Search (AMDS), and two more approximate algorithms: Gaussian Mirror Descent Search (G-MDS) and Gaussian Accelerated Mirror Descent Search (G-AMDS). This research shows that the advanced methods developed in the context of the mirror descent research can be applied to reinforcement learning problem. We also clarify the relationship between an existing reinforcement learning algorithm and our method. With two evaluation experiments, we show our proposed algorithms converge faster than some state-of-the-art methods.

Keywords: Reinforcement Learning, Mirror Descent, Bregman Divergence, Accelerated Mirror Descent, Policy Improvement with Path Integrals

1. Introduction

Similarity between black-box optimization problem and reinforcement learning (RL) problem inspires recent researchers to develop novel RL algorithms [1, 2, 3]. The objective of a black box optimization problem is to find the optimal input $x^* \in \mathcal{X}$ of an unknown function $f : \mathcal{X} \rightarrow \mathbb{R}$. Because the objective function f is unknown, we usually solve the black box optimization problem without gradient information $\nabla_x f$. Such is the case with RL problem. The objective of an RL problem is to find the optimal policy that maximizes the expected cumulative reward [4]. As is the case in a black-box optimization problem, the agent doesn't know the problem formulation initially, so he is required to tackle the lack of

[☆]The research was partially supported by JSPS KAKENHI (Grant numbers JP26120005, JP16H03219, and JP17K12737).

information. In this research, we propose RL algorithms from a standpoint of a black-box optimization problem.

RL algorithm has been categorized into a value-based method and a policy-based method, roughly. In the value-based method, the agent learns the value function of some action in some state. On the other hand, in the policy-based method, the agent learns policy from the observation directly. Moreover, RL algorithm has been divided into a model-free approach and a model-based approach. In the model-based approach, first, the agent gains the model of a system from the sample. Then, it learns policy or the value using the model. In contrast, in the model-free approach, the agent learns the policy or value without the model. RL algorithms usually employ the assumption that the behavior of environment is well approximated by Markov Decision Process (MDP).

Recently, KL divergence regularization plays a key role in policy search algorithms. KL divergence is one of the essential metrics between two distributions. Past methods [5, 6, 7, 8, 9, 10] employ KL divergence regularization to find a suitable distance between a new distribution and a referential distribution. It is important to note that there exists two types of KL divergence: KL and reverse-KL (RKL) divergence [11, 12]. The past researches mentioned above are clearly divided into the algorithms with KL divergence [5, 7] and RKL divergence [6, 8, 9, 10]. We review details of these algorithms afterward.

Bregman divergence is the general metric which includes both of KL and RKL divergence [13] (see Appendix A). Moreover, it includes Euclidean distance, Mahalanobis distance, Hellinger distance and so on. Mirror Descent (MD) algorithm employs the Bregman divergence to regularize the learning steps of decision variables; it includes a variety of gradient methods [14]. Accelerated mirror descent [15] is one of the recent advance applicable for the MD algorithms universally.

In this study, we propose four reinforcement learning algorithms on the basis of MD method. Proposed algorithms can be applied in the non-MDP setting. We propose two essential algorithms and two approximate algorithms of them. We propose mirror descent search (MDS) and accelerated mirror descent search (AMDS) as the essential algorithms, and Gaussian mirror descent search (G-MDS) and Gaussian accelerated mirror descent search (G-AMDS) as the approximate algorithms. G-AMDS showed significant improvement in convergence speed and optimality in two benchmark problems. If other existing reinforcement learning algorithms can be reformulated as the MDS form, they would also get the benefit from the acceleration. We also clarify the relationship between existing reinforcement learning algorithms and our method. As an example, we show the relationship between MDS and Policy Improvement with Path Integrals (PI²) [16, 17] in section 5.

2. Related Works

This section will proceed in the order described below. First of all, we introduce the concept of KL and RKL divergences. Then we refer the two types of RL algorithms: RL with KL divergence [5, 7] and RL with RKL divergence [6, 8, 9, 10]. We also refer the RL algorithm PI²; we show the relation between PI² and our method afterward. We conclude this section with a comment on other MD-based RL algorithms.

The KL divergence between \mathbf{x} and \mathbf{x}' is represented as follows.

$$\text{KL}(\mathbf{x}, \mathbf{x}') = \sum_{j=1}^m x_j \log \frac{x_j}{x'_j} (\mathbf{x}, \mathbf{x}' \in \mathbb{R}^m, x_j, x'_j > 0). \quad (1)$$

We call $\text{KL}(\mathbf{x}', \mathbf{x})$ Kullback Leibler divergence under the condition that we determine \mathbf{x} by reference to the fixed \mathbf{x}' ; we call $\text{KL}(\mathbf{x}, \mathbf{x}')$ reverse-KL divergence [12]. Bregman divergence includes both of KL and RKL divergence [13], so we expect it provides an unified formulation of above-mentioned algorithms.

Let us introduce the RKL-based RL algorithms. Relative Entropy Policy Search (REPS) [6] is one of the pioneering algorithms focusing on the information loss during the policy search process. The information loss is defined as the relative entropy, also known as the RKL divergence, between the old policy and the new policy. The new policy is determined under the upper bound constraints of the RKL divergence. Episode-based REPS also considers information loss bound with regard to the upper-level policy [10]. The method is proposed as an extension of REPS to be an episode-based algorithm. The paper [9] discussed the similarity between Episode-based REPS and the proximal point algorithm; they proposed the Online-REPS algorithm as an theoretically guaranteed one. Model-based Relative Entropy stochastic search (MORE) also employed RKL divergence [8], which extends the episode-based REPS to be a model-based RL algorithm. These algorithms employ RKL divergence in their formulation.

There are some methods employing KL divergence. Trust Region Policy Optimization (TRPO) [5], which is one of the suitable algorithms to solve deep reinforcement learning problem, updates the policy parameters under the KL divergence bound. The research [7] showed that KL divergence between policies plays a key role to derive the well-known heuristic algorithm: Co-variance Matrix Adaptation Evolutionary Strategy (CMA-ES) [18]. Authors named the method Trust-Region Co-variance Matrix Adaptation Evolution Strategy (TR-CMA-ES). TR-CMA-ES is similar to episode-based REPS but uses the KL divergence. Proximal Policy optimization (PPO) algorithm also introduces KL divergence in their penalized objective [19].

PI² [17, 20] would be one of the worth mentioning RL algorithm. PI² encouraged researchers [21, 2] to focus on the relationship between RL algorithms and black box optimization. For example, [21] proposes a reinforcement learning algorithm PI^{BB} on the basis of black box optimization algorithm: CMA-ES. The authors [22, 20] discussed the connection between PI² and KL control. We further discuss PI² from a viewpoint of our proposed methods at section 5.

Previous studies also proposed reinforcement learning algorithms on the basis of MD method [23, 24]. Mirror Descent TD(λ) (MDTD) [23] is a value based RL algorithm. The paper [23] employs Minkowski distance with Euclidean space rather than KL divergence. By contrast, we basically employ the Bregman divergences on the simplex space, i.e. non-Euclidean space. Mirror Descent Guided Policy Search (MDGPS) [24] is also associated with our proposed method. They showed mirror descent formulation improved the Guided Policy Search (GPS) [25]. MDGPS has a distinctive feature that it depends both on KL

divergence and RKL divergence. However, as is shown in [26], there are the variety of Bregman divergences on simplex space other than KL divergence and RKL divergence. Moreover, it plays an important role in accelerating the mirror descent [15]. So we explicitly use Bregman divergence in this research.

3. Mirror Descent Search and Its Variants

3.1. Problem Statement

In this section, we mainly explain our algorithm as a method for the black box optimization problem. Consider the problem of minimizing the original objective function J defined on subspace $\Omega \subseteq \mathbb{R}^l$, i.e. $J : \Omega \rightarrow \mathbb{R}$. We represent the decision variable by $\boldsymbol{\omega} \in \Omega$. Rather than dealing with decision variable $\boldsymbol{\omega} \in \Omega$ directly, we consider the continuous probability density function of $\boldsymbol{\omega}$. Let us introduce the probability space. The probability space is defined as (Ω, \mathcal{F}, P) , where \mathcal{F} is the σ -field of Ω and P is a probability measure over \mathcal{F} .

In this paper, we introduce the continuous probability density function $p(\boldsymbol{\omega})$ as the alternative decision variable defined on the probability space. We also define the alternative objective function by the expectation of the original objective function $J(\boldsymbol{\omega})$:

$$\mathcal{J} = \int_{\Omega} J(\boldsymbol{\omega}) p(\boldsymbol{\omega}) d\boldsymbol{\omega} \quad (2)$$

Therefore, we search the following domain:

$$p(\boldsymbol{\omega}) \geq 0 \quad (3)$$

$$\int_{\Omega} p(\boldsymbol{\omega}) d\boldsymbol{\omega} = 1 \quad (4)$$

Let us introduce the set \mathcal{P}_{all} consists of all probability density functions defined on the probability space. The optimal generative probability is

$$p^*(\boldsymbol{\omega}) = \arg \min_{p(\boldsymbol{\omega}) \in \mathcal{P}_{\text{all}}} \left\{ \int_{\Omega} J(\boldsymbol{\omega}) p(\boldsymbol{\omega}) d\boldsymbol{\omega} \right\} = \arg \min_{p(\boldsymbol{\omega}) \in \mathcal{P}_{\text{all}}} \mathcal{J}. \quad (5)$$

From the viewpoint of the black box optimization problems, the algorithm aims at obtaining the optimal decision variable $p^*(\boldsymbol{\omega})$ to optimize the alternative objective function \mathcal{J} . From the viewpoint of the reinforcement learning problems, it's purpose is to obtain the optimal policy $p^*(\boldsymbol{\omega})$ to optimize reward \mathcal{J} . Next, we introduce an iterative algorithm converges to the optimal solution.

3.2. Mirror Descent Search and Gaussian-Mirror Descent Search

3.2.1. Mirror Descent Search (MDS)

The algorithm is divided into three steps as Fig. 1.

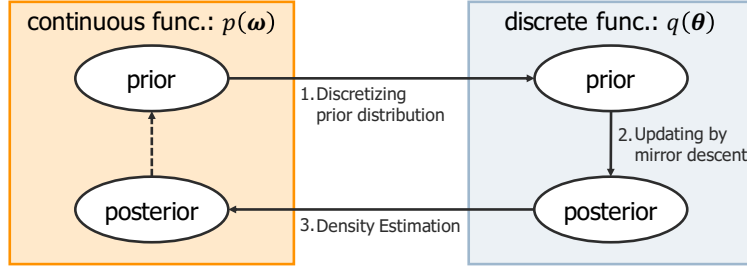


Figure 1: Rough scheme of mirror descent search.

Discretizing Prior Distribution

To update the continuous probability density function $p(\boldsymbol{\omega})$, we need to discretize the probability density function from sampling, because we don't know the form of the objective function. We can only evaluate the objective value corresponding to each sample.

First, we discretize $p(\boldsymbol{\omega})$ based on sampling. For the illustrative purpose, we assume that we can get infinite samples $\boldsymbol{\theta}_i \sim p(\boldsymbol{\omega})$, here. To satisfy the definition of the discrete probability density function, we discretize the continuous distribution p using the function $q: \Omega \rightarrow \mathbb{R}$ for the acquired samples [27]:

$$q(\boldsymbol{\theta}_i) := \lim_{\Delta\boldsymbol{\theta} \rightarrow 0} \frac{p(\boldsymbol{\theta}_i \leq \boldsymbol{\omega} \leq \boldsymbol{\theta}_i + \Delta\boldsymbol{\theta})}{\sum_{j=0}^{\infty} p(\boldsymbol{\theta}_j \leq \boldsymbol{\omega} \leq \boldsymbol{\theta}_j + \Delta\boldsymbol{\theta})} \quad (1 \leq i \leq \infty) \quad (6)$$

$$\sum_{j=0}^{\infty} q(\boldsymbol{\theta}_j) = 1. \quad (7)$$

With Eq. (6) and Eq. (7), our objective function $\tilde{\mathcal{J}}$ becomes the expectation of the original objective function \mathbf{J} :

$$\tilde{\mathcal{J}} = \sum_{j=1}^{\infty} J(\boldsymbol{\theta}_j) q(\boldsymbol{\theta}_j) = \langle \mathbf{J}, \mathbf{q} \rangle, \quad (8)$$

where

$$\mathbf{q} = [q_1, \dots] := [q(\boldsymbol{\theta}_1), \dots] \in \mathcal{Q} \quad (9)$$

$$\mathbf{J} = [J_1, \dots] := [J(\boldsymbol{\theta}_1), \dots] \in \mathbb{R}^{\infty}. \quad (10)$$

Updating by Mirror Descent

After discretizing the continuous distribution $p_{k-1}(\boldsymbol{\omega})$, we employ the mirror descent algorithm (Appendix B) to update the discretized distribution \mathbf{q}_{k-1} :

$$\mathbf{q}_k = \arg \min_{\mathbf{q} \in \mathcal{Q}} \left\{ \langle \nabla_{\mathbf{q}} \tilde{\mathcal{J}}, \mathbf{q} \rangle + \eta B_{\phi}(\mathbf{q}, \mathbf{q}_{k-1}) \right\}, \quad (11)$$

where η is step-size. We call \mathbf{q}_{k-1} as the prior distribution, and \mathbf{q}_k as the posterior distribution. The domain of the decision variable \mathbf{q} is the simplex \mathcal{Q} . B_{ϕ} is the Bregman divergence,

which has an arbitrarily smooth convex function ϕ and is defined as

$$B_\phi(x, x') = \phi(x) - \phi(x') - \langle \nabla \phi(x'), x - x' \rangle. \quad (12)$$

There are numerous variations of Bregman divergence on the simplex such as the KL divergence $\phi(x_k) = \sum_{j=1}^M x_{k,j} \log(x_{k,j})$ and the Euclidean distances assumed on the simplex [26]. Moreover, slightly perturbed KL divergence, which was first introduced in [26], is another important divergence. It plays a key role in accelerating the convergence speed of mirror descent as discussed in [15] and this paper.

Because $\nabla_{\mathbf{q}} \tilde{\mathcal{J}} = \mathbf{J}$, we finally obtain the convex optimization problem:

$$\mathbf{q}_k = \arg \min_{\mathbf{q} \in \mathcal{Q}} \{ \langle \mathbf{J}, \mathbf{q} \rangle + \eta B_\phi(\mathbf{q}, \mathbf{q}_{k-1}) \}. \quad (13)$$

Although we have assumed the infinite number of samples from p , it works only in theory. In what follows, we approximate the distribution \mathbf{q} using sufficiently large m samples.

Density Estimation

We estimate the continuous probability density function $p_k(\boldsymbol{\omega})$ from the posterior distribution \mathbf{q}_k . The procedure of MDS with K -iterations is summarized in Algorithm 1.

Algorithm 1 Mirror descent search

```

1: initialize
   continuous functions:  $p_0(\boldsymbol{\omega}) := p_{\text{init}}(\boldsymbol{\omega})$ .
2: for  $k = 1$  to  $K$  do
3:   for  $i = 1$  to  $m$  do
4:     Sample parameter  $\boldsymbol{\theta}_i \sim p_{k-1}(\boldsymbol{\omega})$ .
5:     (Discretize  $p_{k-1}$ )  $q_{k-1,i} = q(\boldsymbol{\theta}_i)$ .
6:     (Evaluate)  $J_{k-1,i} = J(\boldsymbol{\theta}_i)$ .
7:   end for
8:    $\hat{\mathbf{q}}_k = \arg \min_{\mathbf{q} \in \mathbb{R}^m} \{ \langle \mathbf{J}_{k-1}, \mathbf{q} \rangle + \eta B_\phi(\mathbf{q}, \mathbf{q}_{k-1}) \}$ .
9:   Estimate continuous functions  $p_k(\boldsymbol{\omega})$  from  $\hat{\mathbf{q}}_k$ .
10: end for

```

3.2.2. Gaussian-Mirror Descent Search (G-MDS)

We consider a specific case where the Bregman divergence B_ϕ in Eq. (11) is the RKL divergence. Then, Eq. (13) can be rewritten as follows:

$$\mathbf{q}_k = \arg \min_{\mathbf{q} \in \mathcal{Q}} \{ \langle \mathbf{J}, \mathbf{q} \rangle + \eta \text{KL}(\mathbf{q}, \mathbf{q}_{k-1}) \}. \quad (14)$$

In G-MDS, we considered $q_{k,i} = q(\boldsymbol{\theta}_{k,i})$ as the Gaussian distribution of the mean $\boldsymbol{\mu}_{k-1} \in \mathbb{R}^l$ and the variance-covariance matrix $\boldsymbol{\Sigma}_{\epsilon_{k-1}} \in \mathbb{R}^{l \times l}$, so $\boldsymbol{\theta}_{k,i}$ is generated accordingly:

$$\boldsymbol{\theta}_{k,i} \sim \mathcal{N}(\boldsymbol{\mu}_{k-1}, \boldsymbol{\Sigma}_{\epsilon_{k-1}}) \quad (15)$$

Because the derived algorithm is an instance of MDS with the constraint that the policy is a Gaussian distribution, we named G-MDS. The procedure of G-MDS with K -iterations is summarized in Algorithm 2.

As shown in section 5 and section 4, we discuss G-MDS formulation sheds new light on the existing method PI². Deisenroth also discussed the similarity between episode-based REPS and PI²[28]. To compare the asymptotic behavior of these algorithms appropriately, Algorithm 2 only update the mean vector of Gaussian distribution as PI² also only updates the mean vector. A lot of past studies proposed the procedure to update variance-covariance matrix [18, 29, 7]. These methods would be applicable to the G-MDS.

Algorithm 2 Gaussian mirror descent search

```

1: initialize
   continuous Gaussian function:  $p_0(\boldsymbol{\omega}) := p_{\text{init.}}(\boldsymbol{\omega})$ 
   variance:  $\boldsymbol{\Sigma}$ .
2: for  $k = 1$  to  $K$  do
3:   for  $i = 1$  to  $m$  do
4:     Sample parameter  $\boldsymbol{\theta}_i \sim p_{k-1}(\boldsymbol{\omega})$ .
5:     (Discretize  $p_{k-1}$ )  $q_{k-1,i} = q(\boldsymbol{\theta}_i)$ .
6:     (Evaluate)  $J_{k-1,i} = J(\boldsymbol{\theta}_i)$ .
7:   end for
8:    $\hat{\mathbf{q}}_k = \arg \min_{\mathbf{q} \in \mathbb{R}^m} \{ \langle \mathbf{J}_{k-1}, \mathbf{q} \rangle + \eta \text{KL}(\mathbf{q}, \mathbf{q}_{k-1}) \}$ .
9:   Estimate the mean  $\tilde{\boldsymbol{\mu}}_k$  from  $\hat{\mathbf{q}}_k$ .
10:  Generate continuous function  $p_k(\boldsymbol{\omega})$  from  $\boldsymbol{\mu}_k$  and  $\boldsymbol{\Sigma}$ .
11: end for

```

3.3. Accelerated Mirror Descent Search and Gaussian-Accelerated Mirror Descent Search

3.3.1. Accelerated Mirror Descent Search (AMDS)

Next, the accelerated mirror descent (AMD) method [15] is applied to the proposed method. AMD is an accelerated method that generalizes Nesterov's accelerated gradient such that it can be applied to MD. The details of AMD are explained in Appendix C. Here, AMD yields the following equations:

$$\mathbf{q}_k = \lambda_{k-1} \mathbf{q}_{k-1}^{\tilde{z}} + (1 - \lambda_{k-1}) \mathbf{q}_{k-1}^{\tilde{x}}, \text{ with } \lambda_{k-1} = \frac{r}{r + (k-1)} \quad (16)$$

$$\mathbf{q}_k^{\tilde{z}} = \arg \min_{\mathbf{q}^{\tilde{z}} \in \mathbb{R}^m} \left\{ \frac{(k-1)s}{r} \langle \mathbf{J}_{k-1}, \mathbf{q}^{\tilde{z}} \rangle + B_\phi(\mathbf{q}^{\tilde{z}}, \mathbf{q}_{k-1}^{\tilde{z}}) \right\} \quad (17)$$

$$\mathbf{q}_k^{\tilde{x}} = \arg \min_{\mathbf{q}^{\tilde{x}} \in \mathbb{R}^m} \{ \gamma s \langle \mathbf{J}_{k-1}, \mathbf{q}^{\tilde{x}} \rangle + R(\mathbf{q}^{\tilde{x}}, \mathbf{q}_k) \} \quad (18)$$

where R is regularization function, which belongs to the Bregman divergence [15], r and γ are hyper parameters, and s is step-size.

The procedure of AMDS with K -iterations is summarized in Algorithm 3. Fig. 2 also explains the implementation of AMDS. Each captions in Fig. 2 correspond to the line number of Algorithm 3.

Algorithm 3 Accelerated mirror descent search

```

1: initialize
   continuous functions:  $p_0^{\tilde{z}}(\boldsymbol{\omega}) := p_{\text{init.}}^{\tilde{z}}(\boldsymbol{\omega}), p_0^{\tilde{x}}(\boldsymbol{\omega}) := p_{\text{init.}}^{\tilde{x}}(\boldsymbol{\omega})$ .
2: for  $k = 1$  to  $K$  do
3:    $p_k(\boldsymbol{\omega}) = \lambda_{k-1} p_{k-1}^{\tilde{z}}(\boldsymbol{\omega}) + (1 - \lambda_{k-1}) p_{k-1}^{\tilde{x}}(\boldsymbol{\omega})$ , with  $\lambda_{k-1} = \frac{r}{r+(k-1)}$ .
4:   for  $i = 1$  to  $m$  do
5:     Sample parameter  $\boldsymbol{\theta}_i \sim p_k(\boldsymbol{\omega})$ .
6:     (Discretize  $p_{k-1}^{\tilde{z}}$ )  $q_{k-1,i}^{\tilde{z}} = p_{k-1}^{\tilde{z}}(\boldsymbol{\theta}_i)$ .
7:     (Discretize  $p_{k-1}^{\tilde{x}}$ )  $q_{k-1,i}^{\tilde{x}} = p_{k-1}^{\tilde{x}}(\boldsymbol{\theta}_i)$ .
8:     (Evaluate)  $J_{k-1,i} = J(\boldsymbol{\theta}_i)$ .
9:   end for
10:   $\mathbf{q}_k = \lambda_{k-1} \mathbf{q}_{k-1}^{\tilde{z}} + (1 - \lambda_{k-1}) \mathbf{q}_{k-1}^{\tilde{x}}$ 
11:   $\hat{\mathbf{q}}_k^{\tilde{z}} = \arg \min_{\mathbf{q}^{\tilde{z}} \in \mathbb{R}^m} \left\{ \frac{(k-1)s}{r} \langle \mathbf{J}_{k-1}, \mathbf{q}^{\tilde{z}} \rangle + B_\phi(\mathbf{q}^{\tilde{z}}, \mathbf{q}_{k-1}^{\tilde{z}}) \right\}$ 
12:   $\hat{\mathbf{q}}_k^{\tilde{x}} = \arg \min_{\mathbf{q}^{\tilde{x}} \in \mathbb{R}^m} \left\{ \gamma s \langle \mathbf{J}_{k-1}, \mathbf{q}^{\tilde{x}} \rangle + R(\mathbf{q}^{\tilde{x}}, \mathbf{q}_k) \right\}$ 
13:  Estimate continuous functions  $p_k^{\tilde{z}}(\boldsymbol{\omega}), p_k^{\tilde{x}}(\boldsymbol{\omega})$  from  $\hat{\mathbf{q}}_k^{\tilde{z}}, \hat{\mathbf{q}}_k^{\tilde{x}}$ .
14: end for

```

3.3.2. Gaussian-Accelerated Mirror Descent Search (G-AMDS)

In accordance with prior work [15], we applied the RKL distance to the Bregman divergence B_ϕ in Eq. (17) and $\psi(x) = \varepsilon \sum_{i=1}^n (x_i + \varepsilon) \log(x_i + \varepsilon)$ ($\mathbf{x} \in \mathbb{R}^m, x_{i,j} > 0$) on $R = B_\psi$ in Eq. (18). As the divergence R takes the form of slightly perturbed KL divergence, we represent R by KL_ε in Algorithm 4. We approximate the distributions $p^{\tilde{x}}(\boldsymbol{\theta})$ and $p^{\tilde{z}}(\boldsymbol{\theta})$ with a Gaussian distribution. Accordingly, this method is called G-AMDS. Although the result cannot be calculated analytically, it is known that an efficient numerical calculation of $\mathcal{O}(m \log m)$ time is available[15]. The procedure of G-AMDS with K -iterations is summarized in Algorithm 4.

4. Experimental Evaluations

In this section, we show the comparative experiments. We compare the learning curves of G-MDS, G-AMDS, PI² and episode-based REPS in two tasks. We selected PI² and episode-based REPS as the baseline because they are state-of-the-art methods. In [16, 17], these methods equipped the heuristics such as the normalization of the costs and the simulated annealing. However, in our evaluations, we do not use these heuristics. We focus on the theoretical guaranteed performance of these algorithms. Our source code is available online¹.

¹<https://github.com/mmilk1231/MirrorDescentSearch> We acknowledge with appreciation that PI² code² [16] and the AMD code³ [15] are gratefully helpful to implement our code.

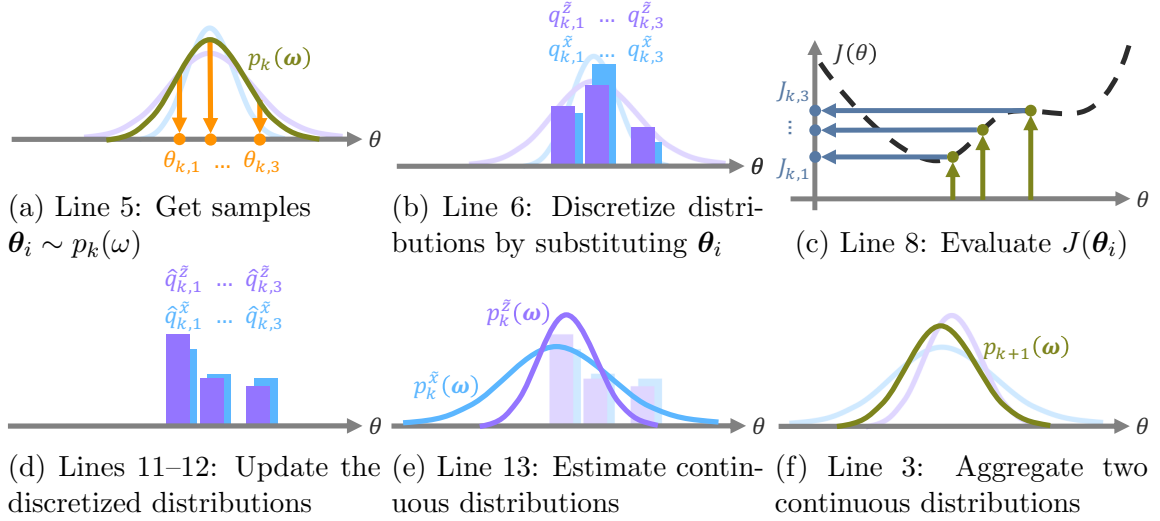


Figure 2: Visualization of Algorithm 3

4.1. 2DOF Point Via-point Task

We performed a 2DOF point via-point task to evaluate the proposed method. The agent is represented as a point on the x–y plane. This agent learns to pass through the point (0.5, 0.2) at 250 ms. We employed DMP [30] to parameterize the policy. DMP represents the trajectory of agent behavior toward x-axis and y-axis in each time step. The parameter settings are as follows: 100 updates, 10 rollouts, and 20 basis functions. Before learning, an initial trajectory from (0, 0) to (1, 1) is generated.

The reward function is as follows:

$$r_t = 5000f_t^2 + 0.5\theta^T\theta \quad (19)$$

$$\Delta r_{250\text{ms}} = 1.0 \times 10^{10} \left((0.5 - x_{250\text{ms}})^2 + (0.2 - y_{250\text{ms}})^2 \right), \quad (20)$$

where $\theta \in \mathbb{R}^{20}$ denotes the policy parameter.

We summarize the results in Fig. 3. Fig. 3a shows that G-AMDS agent learns faster than all the other agents. Fig. 3b shows that the agent was able to accomplish the task.

Table 1 shows the average cost and the standard deviation of the cost at the last update (right-endpoint of Fig. 3a). In the figure, the thin line represents a standard deviation of the cost ($\pm\sigma$). Fig. 3b shows the acquired trajectory at the last update. We set the variance-covariance matrix of sampling distribution to the unit matrix in all algorithms.

²<http://www-clmc.usc.edu/software/git/gitweb.cgi?p=matlab/pi2.git>

³<https://github.com/walidk/AcceleratedMirrorDescent>

Algorithm 4 Gaussian accelerated mirror descent search

```

1: initialize
   continuous Gaussian functions:
    $p_0^{\tilde{z}}(\boldsymbol{\omega}) := p_{\text{init.}}^{\tilde{z}}(\boldsymbol{\omega}), p_0^{\tilde{x}}(\boldsymbol{\omega}) := p_{\text{init.}}^{\tilde{x}}(\boldsymbol{\omega})$ .
   variance:  $\boldsymbol{\Sigma}^{\tilde{z}}, \boldsymbol{\Sigma}^{\tilde{x}}$ .
2: for  $k = 1$  to  $K$  do
3:    $p_k(\boldsymbol{\omega}) = \lambda_{k-1} p_{k-1}^{\tilde{z}}(\boldsymbol{\omega}) + (1 - \lambda_{k-1}) p_{k-1}^{\tilde{x}}(\boldsymbol{\omega})$ , with  $\lambda_{k-1} = \frac{r}{r+(k-1)}$ .
4:   for  $i = 1$  to  $m$  do
5:     Sample parameter  $\boldsymbol{\theta}_i \sim p_k(\boldsymbol{\omega})$ .
6:     (Discretize  $p_{k-1}^{\tilde{z}}$ )  $q_{k-1,i}^{\tilde{z}} = p_{k-1}^{\tilde{z}}(\boldsymbol{\theta}_i)$ .
7:     (Discretize  $p_{k-1}^{\tilde{x}}$ )  $q_{k-1,i}^{\tilde{x}} = p_{k-1}^{\tilde{x}}(\boldsymbol{\theta}_i)$ .
8:     (Evaluate)  $J_{k-1,i} = J(\boldsymbol{\theta}_i)$ .
9:   end for
10:   $\mathbf{q}_k = \lambda_{k-1} \mathbf{q}_{k-1}^{\tilde{z}} + (1 - \lambda_{k-1}) \mathbf{q}_{k-1}^{\tilde{x}}$ 
11:   $\hat{\mathbf{q}}_k^{\tilde{z}} = \arg \min_{\mathbf{q}^{\tilde{z}} \in \mathbb{R}^m} \left\{ \frac{(k-1)s}{r} \langle \mathbf{J}_{k-1}, \mathbf{q}^{\tilde{z}} \rangle + \text{KL}(\mathbf{q}^{\tilde{z}}, \mathbf{q}_{k-1}^{\tilde{z}}) \right\}$ 
12:   $\hat{\mathbf{q}}_k^{\tilde{x}} = \arg \min_{\mathbf{q}^{\tilde{x}} \in \mathbb{R}^m} \left\{ \gamma s \langle \mathbf{J}_{k-1}, \mathbf{q}^{\tilde{x}} \rangle + \text{KL}_\varepsilon(\mathbf{q}^{\tilde{x}}, \mathbf{q}_k) \right\}$ 
13:  Estimate the means  $\boldsymbol{\mu}_k^{\tilde{z}}, \boldsymbol{\mu}_k^{\tilde{x}}$  from  $\hat{\mathbf{q}}_k^{\tilde{z}}, \hat{\mathbf{q}}_k^{\tilde{x}}$ .
14:  Generate continuous functions  $p_k^{\tilde{z}}(\boldsymbol{\omega}), p_k^{\tilde{x}}(\boldsymbol{\omega})$  from  $\boldsymbol{\mu}_k^{\tilde{z}}, \boldsymbol{\mu}_k^{\tilde{x}}, \boldsymbol{\Sigma}^{\tilde{z}}, \boldsymbol{\Sigma}^{\tilde{x}}$ .
15: end for

```

4.2. 10DOF Arm Via-point Task and 50DOF Arm Via-point Task

We performed a 10DOF arm via-point task and a 50DOF arm via-point task to evaluate the proposed method. The agent learns to control his end-effector to pass through the point (0.5, 0.5) at 300 ms. Before learning, arm trajectory is initialized to minimize the jerk.

The reward function with the D [DOF] arm is as follows:

$$r_t = \frac{\sum_{i=1}^D (D+1-i) (0.1 f_{i,t}^2 + 0.5 \theta_i^T \theta_i)}{\sum_{i=1}^D (D+1-i)} \quad (21)$$

$$\Delta r_{300\text{ms}} = 1.0 \times 10^8 \left((0.5 - x_{300\text{ms}})^2 + (0.5 - y_{300\text{ms}})^2 \right) \quad (22)$$

Table 1: Final cost of 2DOF point via-point task

| | |
|--------------------|---------------------------------------|
| G-AMDS | $1.3 \times 10^7 \pm 1.0 \times 10^6$ |
| G-MDS | $4.9 \times 10^7 \pm 8.3 \times 10^6$ |
| PI ² | $1.6 \times 10^9 \pm 4.1 \times 10^7$ |
| Episode-based REPS | $2.0 \times 10^7 \pm 2.6 \times 10^6$ |

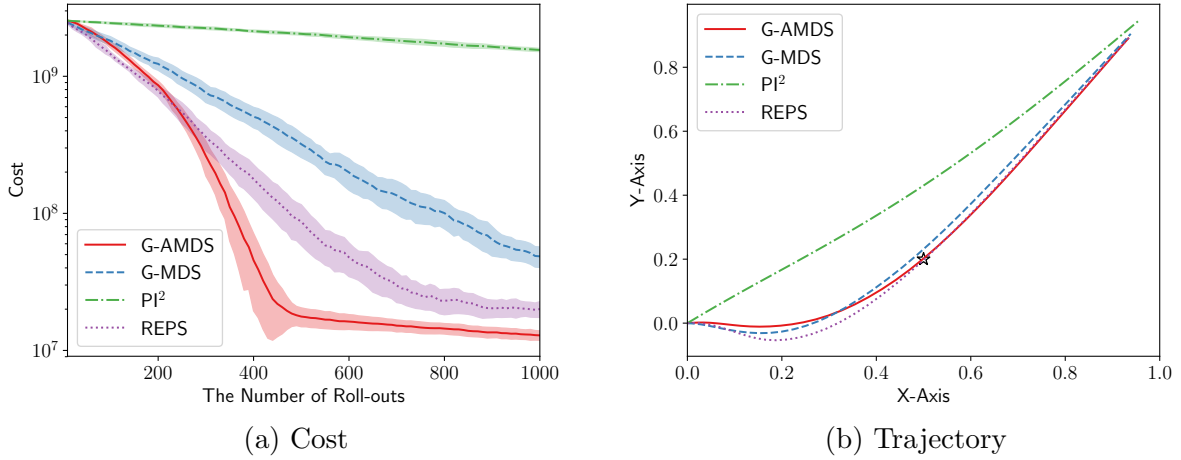


Figure 3: 2DOF point via-point task

, where x_t and y_t are the end-effector position. DMP [30] is also used to parameterize the policy. The parameter settings are as follows: 1000 updates, 10 rollouts, and 100 basis functions.

We summarize the results in Fig. 4 and Fig. 5. From Fig. 4a and Fig. 5a, we can confirm that G-AMDS learns faster than all the other algorithms. Moreover, the variance of G-AMDS is smallest. As Fig. 4b and Fig. 5b show, it is clear that the G-AMDS agent accomplished both of 10 DOF task and 50 DOF task. Thus, G-AMDS would have scalability for dimensionality.

Table 2 and Table 3 show the average cost and the standard deviation of the cost at the last update.

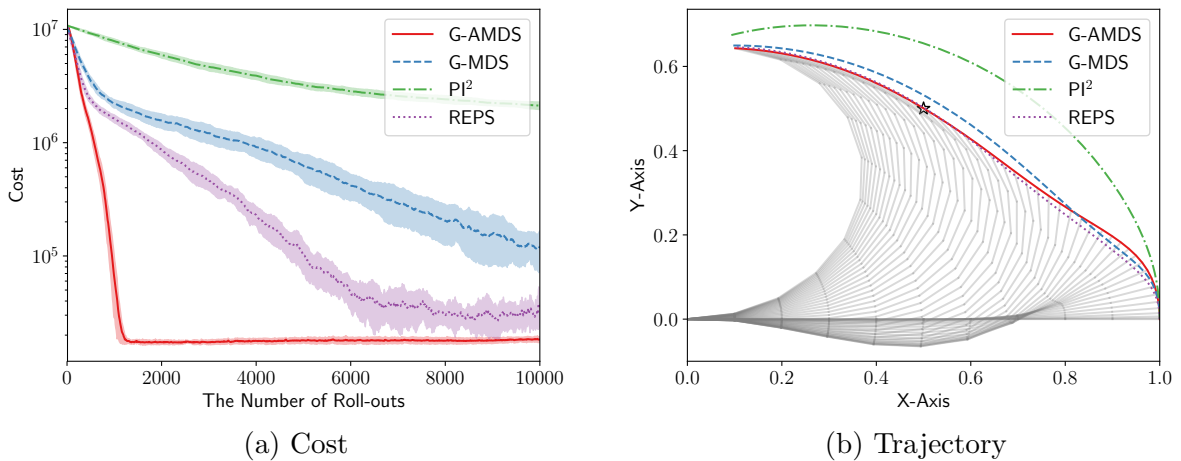


Figure 4: 10DOF arm via-point task

Table 2: Final cost of 10DOF arm via-point task

| | |
|--------------------|---------------------------------------|
| G-AMDS | $1.8 \times 10^4 \pm 1.1 \times 10^3$ |
| G-MDS | $1.2 \times 10^5 \pm 4.6 \times 10^4$ |
| PI ² | $2.1 \times 10^6 \pm 1.6 \times 10^5$ |
| Episode-based REPS | $3.6 \times 10^4 \pm 1.2 \times 10^4$ |

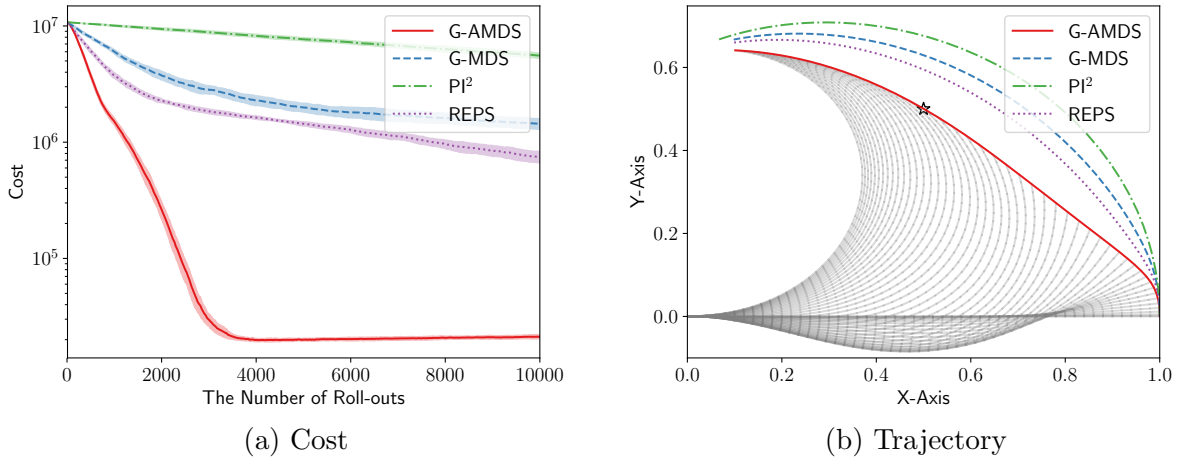


Figure 5: 50DOF arm via-point task

5. Relation between MDS and PI²

Theodorou et al. proposed PI² algorithm in [17] and they discussed the relation between PI² and KL control in [22, 20]. In this section, we provide an explanation of PI² from a viewpoint of MDS.

5.1. Problem Statement and Algorithm of PI²

We begin with the problem statement of PI² [22, 31]:

$$\min_{\{\mathbf{u}_k\}_{k=t, \dots, T}} \mathbf{E}_{\tau}[L(\tau)] \quad (23)$$

$$\text{s.t. } d\mathbf{x}_t = \mathbf{f}(\mathbf{x}_t)dt + \mathbf{G}(\mathbf{x}_t)(\mathbf{u}_tdt + d\mathbf{w}_t), \quad (24)$$

where $\mathbf{x}_t \in \mathbb{R}^n$, $\mathbf{f}(\mathbf{x}_t) \in \mathbb{R}^n$, $\mathbf{G}(\mathbf{x}_t) \in \mathbb{R}^{n \times m}$, $\mathbf{u}_t \in \mathbb{R}^m$ and $\tau := (\mathbf{x}_t, \mathbf{x}_{t+dt}, \dots, \mathbf{x}_T)$. $\mathbf{w}_t \in \mathbb{R}^m$ is Wiener process [31]. It is essential to point out that $\mathbf{u}_tdt + d\mathbf{w}_t$ plays a role as feedback gain of $\mathbf{G}(\mathbf{x}_t)$, so our objective is to find the optimal feedback gain; we try to optimize the averaged continuous time series \mathbf{u}_t especially.

Table 3: Final cost of 50DOF arm via-point task

| | |
|--------------------|---------------------------------------|
| G-AMDS | $2.1 \times 10^4 \pm 8.5 \times 10^2$ |
| G-MDS | $1.4 \times 10^6 \pm 1.5 \times 10^5$ |
| PI ² | $5.6 \times 10^6 \pm 3.0 \times 10^5$ |
| Episode-based REPS | $7.5 \times 10^5 \pm 8.3 \times 10^4$ |

Eq. (24) can be interpreted in two ways. Under the model-free reinforcement learning problem, Eq. (24) represents the actual physical dynamics of the real plant. Under the model-predictive optimal control problem, Eq. (24) would represent the predictive model of the real plant. Essentially, we consider the model-free reinforcement learning setting, below.

Eq. (23)-Eq. (24) satisfies linearized Hamilton-Jacobi-Bellman equation under the quadratic cost assumption $L(\boldsymbol{\tau}) = l(\boldsymbol{\tau}) + \sum_{k=t}^T \mathbf{u}_k^T \mathbf{R} \mathbf{u}_k$ [17, 31]. $l(\boldsymbol{\tau})$ denotes some state dependent cost $l(\boldsymbol{\tau}) := \phi(\mathbf{x}_T) + \sum_{k=t}^{T-1} q(\mathbf{x}_k)$. With the path integral calculation, we acquire the analytic solution of the HJB equation. They finally proposed Algorithm 5 as an iterative algorithm for the problem.

Next, we discuss the relation between MDS and PI². Theodorou et al. [22, 20] proposed more general problem setting, so we touch the subject in section 5.3.

Algorithm 5 PI² algorithm (see [17] for details)

```

1: initialize
   parameter vector:  $\boldsymbol{\theta}_0 := \boldsymbol{\theta}_{\text{init}}$ 
2: for  $k = 1$  to  $K$  do
3:   for  $i = 1$  to  $m$  do
4:     for  $t = 0$  to  $T - 1$  do
5:       Generate rollout from  $\boldsymbol{\theta}_{k-1} + \boldsymbol{\epsilon}_{t,i}$ 
6:       Compute the projection matrix  $\mathbf{M}_{t,k} = \frac{\mathbf{R}^{-1} \mathbf{g}_{t,k} \mathbf{g}_{t,k}^T}{\mathbf{g}_{t,k}^T \mathbf{R}^{-1} \mathbf{g}_{t,k}}$ 
7:       Evaluate  $S(\boldsymbol{\tau}_{t,i}) = \phi + \sum_{j=t}^{T-1} q_{j,k} + \frac{1}{2} (\boldsymbol{\theta}_{k-1} + \mathbf{M}_{j,i} \boldsymbol{\epsilon}_{j,i})^T \mathbf{R} (\boldsymbol{\theta}_{k-1} + \mathbf{M}_{j,i} \boldsymbol{\epsilon}_{j,i})$ 
8:       Compute the probability  $P(\boldsymbol{\tau}_{t,i}) = \exp(-\frac{1}{\lambda} S(\boldsymbol{\tau}_{t,i})) / Z$ 
9:       Compute time dependent differential parameter  $\delta \boldsymbol{\theta}_t = \sum_{i=1}^m [P(\boldsymbol{\tau}_{t,i}) \mathbf{M}_{t,i} \boldsymbol{\epsilon}_{t,i}]$ 
10:    end for
11:    Compute time independent differential parameter  $\delta \boldsymbol{\theta} = \frac{\sum_{j=0}^{T-1} (T-j) \delta \boldsymbol{\theta}_j}{\sum_{j=0}^{T-1} (T-j)}$ 
12:  end for
13:   $\boldsymbol{\theta}_k = \boldsymbol{\theta}_{k-1} + \delta \boldsymbol{\theta}$ 
14: end for

```

5.2. PI^2 from a Viewpoint of MDS

First of all, we reformulate Eq. (23)-Eq. (24) as Eq. (25):

$$\min_{p(\mathbf{h})} \int J(\mathbf{h})p(\mathbf{h})d\mathbf{h}, \quad (25)$$

where $p(\mathbf{h})$ is the probability distribution of the stochastic process $\mathbf{h} := (dz_t, \dots, dz_T)$ with $dz_t = \mathbf{u}_t dt + d\mathbf{w}_t$. Stochastic process \mathbf{h} is the Gaussian process with mean function $\boldsymbol{\mu} := (\mathbf{u}_t dt, \dots, \mathbf{u}_T dt)$ because every increments $d\mathbf{w}_t$ are Gaussian. Once $\mathbf{h}_j \sim p(\mathbf{h})$ is sampled, trajectory $\boldsymbol{\tau}(\mathbf{h}_j)$ and $L(\boldsymbol{\tau}(\mathbf{h}_j))$ are uniquely determined, so we defined $J(\mathbf{h}) := L(\boldsymbol{\tau}(\mathbf{h}))$. Our problem is to find the optimal probability distribution $p^*(\mathbf{h})$.

We introduce MDS approach to optimize $p(\mathbf{h})$:

$$p_{k+1}(\mathbf{h}) = \arg \min_{p(\mathbf{h})} \left\{ \int J(\mathbf{h})p(\mathbf{h})d\mathbf{h} + \eta \text{KL}[p(\mathbf{h}) | p_k(\mathbf{h})] \right\}. \quad (26)$$

Eq. (27) is the solution of Eq. (26), which is also known as exponentiated gradient [32].

$$p_{k+1}(\mathbf{h}) = \frac{\exp(-\frac{1}{\eta}J(\mathbf{h}))p_k(\mathbf{h})}{\int \exp(-\frac{1}{\eta}J(\mathbf{h}))p_k(\mathbf{h})d\mathbf{h}} \quad (27)$$

The posterior mean function becomes

$$\boldsymbol{\mu}_{k+1} = \int \mathbf{h} \cdot p_{k+1}(\mathbf{h})d\mathbf{h} \quad (28)$$

$$= \frac{\int \mathbf{h} \exp(-\frac{1}{\eta}J(\mathbf{h}))p_k(\mathbf{h})d\mathbf{h}}{\int \exp(-\frac{1}{\eta}J(\mathbf{h}))p_k(\mathbf{h})d\mathbf{h}}. \quad (29)$$

By the Monte Carlo approximation, Eq. (29) can be approximated by

$$\tilde{\boldsymbol{\mu}}_{k+1} = \boldsymbol{\mu}_k + \frac{\sum_{j=1}^m (\mathbf{h}_j - \boldsymbol{\mu}_k) \exp(-\frac{1}{\eta}J(\mathbf{h}_j))}{\sum_{j=1}^m \exp(-\frac{1}{\eta}J(\mathbf{h}_j))} \quad (30)$$

where $\mathbf{h}_j - \boldsymbol{\mu}_k = (d\mathbf{w}_{t,j}, \dots, d\mathbf{w}_{T,j})$. With the above mentioned procedure, $p(\mathbf{h})$ gradually gets closer to the optimal $p^*(\mathbf{h})$.

We explain the similarity and difference between Eq. (30) and PI^2 . To simplify the notations, we introduce $\boldsymbol{\varepsilon}_{k,j} := (\mathbf{h}_j - \boldsymbol{\mu}_k)$. Eq. (30) becomes

$$\tilde{\boldsymbol{\mu}}_{k+1} = \boldsymbol{\mu}_k + \sum_{j=1}^m \boldsymbol{\varepsilon}_{k,j} P_{k,j} \quad (31)$$

$$P_{k,j} := \frac{\exp(-\frac{1}{\eta}J(\mathbf{h}_j))}{\sum_{j=1}^m \exp(-\frac{1}{\eta}J(\mathbf{h}_j))} \quad (32)$$

Eq. (31)-Eq. (32) correspond to Line 9-13 in Algorithm 5. There are two important differences between PI^2 and the algorithms obtained here. First, as Line 7-9 in Algorithm 5 show, PI^2 sequentially updates the decision variable $\boldsymbol{\mu}_k$ at each time step t based on the provisional cumulative rewards $(S(\boldsymbol{\tau}_{t,1}), \dots, S(\boldsymbol{\tau}_{t,m}))$. On the other hand, as Eq. (31) shows, our procedure just uses the entire cumulative rewards. We can bridge the gap by introducing Dynamic Programming as used in [22, 20] (see Appendix E). Second, PI^2 assumes a Wiener process, but MDS is applicable for arbitrary stochastic processes. This difference would be important to deal with more complex stochastic processes.

5.3. More General Problem Setting and Online Mirror Descent Trick

Theodorou et al. proposed more general problem setting in [22, 20].

$$\min_{\{\mathbf{u}_k\}_{k=t,\dots,T}} \mathbf{E}_{\boldsymbol{\tau}}[L(\boldsymbol{\tau})] \quad (33)$$

$$\text{s.t.} \quad d\mathbf{x}_t = \mathbf{f}(\mathbf{x}_t)dt + \mathbf{G}(\mathbf{x}_t)(d\mathbf{z}_t + d\boldsymbol{\xi}_t) \quad (34)$$

$$d\mathbf{z}_t = \mathbf{u}_t dt + d\mathbf{w}_t. \quad (35)$$

They introduced additional wiener process $d\boldsymbol{\xi}_t$ which represents the stochasticity of passive dynamics. All the other variables are defined in section 5.1 and section 5.2.

In this setting, trajectory $\boldsymbol{\tau}$ becomes stochastic variable even after $\mathbf{h}_j = (d\mathbf{z}_t, \dots, d\mathbf{z}_T)$ is sampled. The evaluated value $J(\mathbf{h})$ is represented by

$$J(\mathbf{h}) = \int p(\boldsymbol{\xi}) j(\mathbf{h}, \boldsymbol{\xi}) d\boldsymbol{\xi}, \quad (36)$$

with $j(\mathbf{h}, \boldsymbol{\xi}) := L(\boldsymbol{\tau}(\mathbf{h}, \boldsymbol{\xi}))$.

It is important to note that we can approximate MDS by:

$$p_{k+1}(\mathbf{h}) = \arg \min_{p \in \mathcal{P}} \left\{ \int j(\mathbf{h}, \boldsymbol{\xi}_k) p(\mathbf{h}) d\mathbf{h} + \eta B_{\phi}(p(\mathbf{h}), p_k(\mathbf{h})) \right\}, \quad (37)$$

$$\text{s.t.} \quad J(\mathbf{h}) = \lim_{k \rightarrow \infty} \frac{1}{k} \sum_k j(\mathbf{h}, \boldsymbol{\xi}_k) \quad (38)$$

We can prove that Eq. (37) will asymptotically converge to the optimal solution (see Appendix D). This trick is called online mirror descent. It enables us to make use of MDS under a single roll-out setting. Fig. 6 is the schematic view of Eq. (36) and Eq. (38).

Such is the case with reinforcement learning problem. We usually employ the expected cumulative reward as the objective function $J(\mathbf{h})$. Although there exist not only uncertainty in the dynamics but also in the reward function, we expect Eq. (37) is applicable for the reinforcement learning problems.

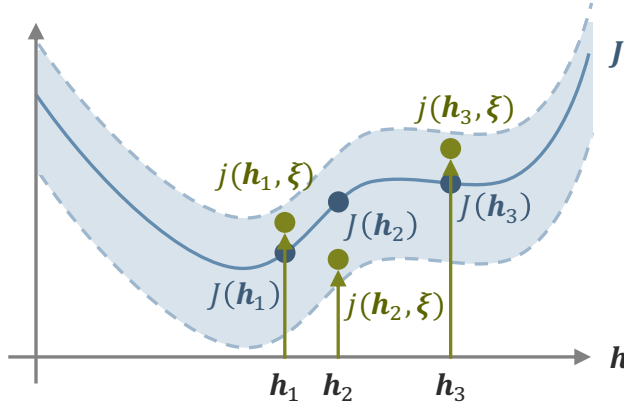


Figure 6: The problem setting that evaluation value $J(\mathbf{h})$ is represented as an expectation of $j(\mathbf{h}, \xi)$.

6. Conclusions

In this research, we proposed four optimization algorithms both for black-box optimization problem and reinforcement learning problem. On the basis of MD method, we proposed two essential algorithms: MDS and AMDS. Moreover, we proposed two more approximate algorithms of them: G-MDS and G-AMDS. Then, we discussed the relation between our proposed methods and the related algorithms. Especially in section 5, we provided the detailed discussion about the relation between MDS and PI^2 . We compared the performances of G-MDS, G-AMDS, PI^2 and episode-based REPS in two tasks. G-AMDS showed significant improvements in convergence speed and optimality.

These results suggest that variety of existing MD extensions can be applied to reinforcement learning algorithms. Moreover, it would be also possible that variety of Bayesian techniques such as variational inference are applicable to reinforcement learning algorithms as there exists the theoretical relation between MD method and Bayes theorem [33]. We refer to Natural Evolution Strategies (NES) [34, 3]. NES uses the natural gradient to update the parameterized distribution. Natural gradient comes from the constraints on KL divergence or Hellinger distance between two distributions. Because Bregman divergence includes both KL and Hellinger distance, we expect there exists some connections between MDS and NES. Recent work suggests that the relation exists between the natural gradient and the MD [35]. Although we didn't evaluate G-MDS and G-AMDS with the variance-covariance matrix update in this study, we believe CMA-ES and its variants would improve performance. Parallelization of MDS algorithms would also be important work.

Acknowledgment

The research was supported by JSPS KAKENHI (Grant numbers JP26120005, JP16H03219, and JP17K12737).

Appendix A. Bregman, KL and RKL divergence

We sketch the proof that both of KL and RKL divergence are Bregman divergence [13].

First of all, we define the smooth convex function $\phi(\mathbf{x})$ in the Bregman divergence Eq. (12) as

$$\phi_\alpha(\mathbf{x}) = \frac{2}{1+\alpha} \sum_{i=1}^N \left(1 + \frac{1-\alpha}{2} x_i\right)^{\frac{2}{1-\alpha}}, \quad (\text{A.1})$$

where $\mathbf{x} \in \mathbb{R}^N$, $x_i > 0$ and $\alpha \neq \pm 1$. By directly substituting Eq. (A.1) into the Bregman divergence, we acquire B_α . The work [13] provides the proof that B_α becomes α -divergence. The divergence under $\alpha = \pm 1$ condition is defined by a limit case $\alpha \rightarrow \pm 1$.

The limit case $\alpha \rightarrow \pm 1$ of B_α is easy to calculate. We acquire

$$\lim_{\alpha \rightarrow +1} B_\alpha(\mathbf{x}, \mathbf{y}) = \sum_i^N \left[\exp(x_i) - \exp(y_i) + \exp(y_i) (y_i - x_i) \right], \quad (\text{A.2})$$

and

$$\lim_{\alpha \rightarrow -1} B_\alpha(\mathbf{x}, \mathbf{y}) = \sum_i^N \left[-x_i + y_i + (1+x_i) \log(1+x_i) - (1+x_i) \log(1+y_i) \right]. \quad (\text{A.3})$$

Under the conditions $x_i = \log p_i$ and $y_i = \log q_i$, Eq. (A.2) becomes

$$\lim_{\alpha \rightarrow 1} B_\alpha(\log \mathbf{p}, \log \mathbf{q}) = \sum_i^N q_i \log \frac{q_i}{p_i}, \quad (\text{A.4})$$

and, under the conditions $x_i = p_i - 1$ and $y_i = q_i - 1$, Eq. (A.3) becomes

$$\lim_{\alpha \rightarrow -1} B_\alpha(\mathbf{p} - 1, \mathbf{q} - 1) = \sum_i^N p_i \log \frac{p_i}{q_i}. \quad (\text{A.5})$$

Here, we used $\sum p_i = \sum q_i = 1$ in these calculation.

Finally, we proved both of KL and RKL divergences belongs to Bregman divergence as is shown by Eq. (A.4) and Eq. (A.5).

Appendix B. Mirror Descent

We explain the mirror descent algorithm in this section. Let $x \in \mathcal{X}$ and $f : \mathcal{X} \rightarrow \mathbb{R}$ be a decision variable and an objective function.

$$x_k = \arg \min_{x \in \mathcal{X}} \{ \langle \nabla f(x_{k-1}), x \rangle + \eta B_\phi(x, x_{k-1}) \} \quad (\text{B.1})$$

, where B_ϕ is the Bregman divergence. The first term linearizes the objective function $f(x)$ around $x = x_{k-1}$, and the second term controls the step size of $x \in \mathcal{X}$ by bounding the Bregman divergence between the new decision variable candidate x and old one x_{k-1} .

Appendix C. Accelerated Mirror Descent

We explain the accelerated mirror descent (AMD) algorithm in this section. This algorithm is proposed in [15]. The AMD is an accelerated method that generalizes Nesterov's accelerated gradient descent. Let $x \in \mathcal{X}$ and $f : \mathcal{X} \rightarrow \mathbb{R}$ be a decision variable and an objective function.

$$x_k = \lambda_{k-1} \tilde{z}^{k-1} + (1 - \lambda_{k-1}) \tilde{x}_{k-1}, \text{ with } \lambda_{k-1} = \frac{r}{r + (k-1)} \quad (\text{C.1})$$

$$\tilde{z}_k = \arg \min_{\tilde{z} \in \mathcal{X}} \left\{ \frac{(k-1)s}{r} \langle \nabla f(x_k), \tilde{z} \rangle + B_\phi(\tilde{z}, \tilde{z}_{k-1}) \right\} \quad (\text{C.2})$$

$$\tilde{x}_k = \arg \min_{\tilde{x} \in \mathcal{X}} \{ \gamma s \langle \nabla f(x_k), \tilde{x} \rangle + R(\tilde{x}, x_k) \}, \quad (\text{C.3})$$

where B_ϕ is the Bregman divergence, r and γ are hyper parameters, and s is step-size. In general, $R(x, x') = B_\omega(x, x')$ represents the Bregman divergence of the arbitrarily smooth convex function $\omega(x)$. For more detail on the algorithm, refer to [15].

AMD consist of two MD equations Eqs. (C.2) and (C.3). Parameter λ in Eq. (C.1) defines the mixture ratio of Eqs. (C.2) and (C.3). λ is initially close to 1, so AMD behaves according to Eq. (C.2). As λ comes close to 0, AMD converges Eq. (C.3).

We provide two topics related to this method. First, AMD naturally includes simulated annealing, while the existing method such as PI² includes it heuristically [16, 17]. Parameter $\frac{(k-1)s}{r}$ in Eq. (C.2) is a time-varying learning rate; as the learning step k proceeds, the factor ∇f becomes increasingly important for the optimization in Eq. (C.2). This is equivalent to a simulated annealing operation. It would be more clear if you reformulate Eq. (C.2) in exponentiated gradient form.

Another topic is about an advantage of reverse-KL (RKL) minimization: $\min_q \text{KL}[q||p]$. The methods in this paper and original AMD paper both include it. The RKL minimization problem shows mode-seeking behavior when p is the multi-modal distribution [11]. According to Eq. (C.1), x_k becomes a multi-modal distribution when \tilde{z}_k and \tilde{x}_k are on simplex space. Such is the case with $R(\tilde{x}, x_k)$ in Eq. (C.3). As the learning step k proceeds, $R(\tilde{x}, x_k)$ gradually becomes to lead \tilde{x} to $x_{k-1}^{\tilde{x}}$ from $z_{k-1}^{\tilde{x}}$. We guess the mode-seeking behavior is effective for the AMD to convert to the latter MD algorithm Eq. (C.3).

Appendix D. Online Mirror Descent

We begin with the optimization problem:

$$\mathbf{q}_k = \arg \min_{\mathbf{q} \in \mathbb{R}^\infty} \{ \langle \mathbf{j}_{k-1}, \mathbf{q} \rangle + \eta B_\phi(\mathbf{q}, \mathbf{q}_{k-1}) \}, \quad (\text{D.1})$$

$$\text{s.t.} \quad \mathbf{J} = \lim_{k \rightarrow \infty} \frac{1}{k} \sum_k \mathbf{j}_k \quad (\text{D.2})$$

From the formula deformation

$$\mathbf{q}_k = \arg \min_{\mathbf{q} \in \mathbb{R}^\infty} \{ \langle \mathbf{j}_{k-1}, \mathbf{q} \rangle + \eta (\phi(\mathbf{q}) - \phi(\mathbf{q}_{k-1}) - \langle \nabla \phi(\mathbf{q}_{k-1}), \mathbf{q} - \mathbf{q}_{k-1} \rangle) \} \quad (\text{D.3})$$

$$= \arg \min_{\mathbf{q} \in \mathbb{R}^\infty} \{ \langle \mathbf{j}_{k-1} - \eta \nabla \phi(\mathbf{q}_{k-1}), \mathbf{q} \rangle + \eta \phi(\mathbf{q}) \}, \quad (\text{D.4})$$

and a relational expression of the dual space in mirror descent

$$\nabla \phi(\mathbf{q}_{k-1}) = \nabla \phi(\mathbf{q}_{k-2}) - \frac{1}{\eta} \mathbf{j}_{k-2} = \dots = \nabla \phi(\mathbf{q}_0) - \frac{1}{\eta} \sum_{i=0}^{k-2} \mathbf{j}_i, \quad (\text{D.5})$$

we can reformulate Eq. (D.1) as follows:

$$\mathbf{q}_k = \arg \min_{\mathbf{q} \in \mathbb{R}^\infty} \left[\langle \mathbf{j}_{k-1} - \eta \left\{ \nabla \phi(\mathbf{q}_0) - \frac{1}{\eta} \sum_{i=0}^{k-2} \mathbf{j}_i \right\}, \mathbf{q} \rangle + \eta \phi(\mathbf{q}) \right] \quad (\text{D.6})$$

$$= \arg \min_{\mathbf{q} \in \mathbb{R}^\infty} \left[\langle \sum_{i=0}^{k-1} \mathbf{j}_i - \eta \nabla \phi(\mathbf{q}_0), \mathbf{q} \rangle + \eta \phi(\mathbf{q}) \right] \quad (\text{D.7})$$

$$= \arg \min_{\mathbf{q} \in \mathbb{R}^\infty} \left[\langle k \cdot \frac{1}{k} \sum_{i=0}^{k-1} \mathbf{j}_i - \eta \nabla \phi(\mathbf{q}_0), \mathbf{q} \rangle + \eta \phi(\mathbf{q}) \right], \quad (\text{D.8})$$

$$= \arg \min_{\mathbf{q} \in \mathbb{R}^\infty} \left[\langle k \hat{\mathbf{J}} - \eta \nabla \phi(\mathbf{q}_0), \mathbf{q} \rangle + \eta \phi(\mathbf{q}) \right] \quad (\text{D.9})$$

Next, we reformulate the original problem in the same way.

$$\mathbf{q}_k = \arg \min_{\mathbf{q} \in \mathbb{R}^\infty} \{ \langle \mathbf{J}, \mathbf{q} \rangle + \eta B_\phi(\mathbf{q}, \mathbf{q}_{k-1}) \}. \quad (\text{D.10})$$

$$= \arg \min_{\mathbf{q} \in \mathbb{R}^\infty} [\langle k \mathbf{J} - \eta \nabla \phi(\mathbf{q}_0), \mathbf{q} \rangle + \eta \phi(\mathbf{q})]. \quad (\text{D.11})$$

The more the number of updates k increases, the more $\hat{\mathbf{J}}$ gets closer to \mathbf{J} . Thus, we can replace \mathbf{J} in Eq. (D.10) with \mathbf{j}_{k-1} , when the number of updates is sufficient.

Appendix E. Dynamic Programming on MDS

We begin with the problem setting:

$$p_{k+1}(\mathbf{h}) = \arg \min_{p(\mathbf{h})} \left\{ \int J(\mathbf{h}) p(\mathbf{h}) d\mathbf{h} + \eta \text{KL}[p(\mathbf{h}) | p_k(\mathbf{h})] \right\}. \quad (\text{E.1})$$

We assume discrete time dynamics and the specific Markov Chain structure [20]:

$$p_k(\mathbf{h}) = \prod_{t=1}^T p_k(h_t | h_{t-1}). \quad (\text{E.2})$$

In addition, we assume the decomposable objective function

$$J(\mathbf{h}) = \sum_{t=0}^T F(h_t). \quad (\text{E.3})$$

Eq. (E.1) becomes

$$p_{k+1}(\mathbf{h}) = \arg \min_{p(\mathbf{h})} \left\{ F(h_0) + \int d\mathbf{h} p(\mathbf{h}) \sum_{t=1}^T \left(F(h_t) + \eta \log \frac{p(h_t | h_{t-1})}{p_k(h_t | h_{t-1})} \right) \right\}. \quad (\text{E.4})$$

By Bellman principle, we get (see [20] for details)

$$V_t(h_t) = \min_{p(h_{t+1}|h_t)} \left\{ F(h_t) + \eta \text{KL}[p(h_{t+1}|h_t) | p_k(h_{t+1}|h_t)] + \int V_{t+1}(h_{t+1}) dp(h_{t+1}|h_t) \right\}. \quad (\text{E.5})$$

Thus we get

$$p_{k+1}(h_{t+1}|h_t) = \frac{\exp(-\frac{1}{\eta} V_{t+1}(h_{t+1})) p_k(h_{t+1}|h_t)}{Z}. \quad (\text{E.6})$$

and finally,

$$\exp(-\frac{1}{\eta} V_{t+1}(h_{t+1})) = \mathbf{E}_{p(h_{k+1}|h_k)} \left[\exp(-\sum_{k=t}^T F(h_k)) \right]. \quad (\text{E.7})$$

References

- [1] F. Stulp, O. Sigaud, Policy improvement: Between black-box optimization and episodic reinforcement learning, in: Journées Francophones Planification, Décision, et Apprentissage pour la conduite de systèmes, France, 2013, pp. 1–15.
URL <https://hal.archives-ouvertes.fr/hal-00922133>
- [2] J. Hwangbo, C. Gehring, H. Sommer, R. Siegwart, J. Buchli, ROCK*- Efficient black-box optimization for policy learning, in: 2014 IEEE-RAS International Conference on Humanoid Robots, IEEE, 2014, pp. 535–540.
- [3] T. Salimans, J. Ho, X. Chen, S. Sidor, I. Sutskever, Evolution Strategies as a Scalable Alternative to Reinforcement Learning, ArXiv e-prints [arXiv:1703.03864](https://arxiv.org/abs/1703.03864).
- [4] R. S. Sutton, A. G. Barto, Reinforcement learning: An introduction, MIT press Cambridge, 1998.
- [5] J. Schulman, S. Levine, P. Abbeel, M. Jordan, P. Moritz, Trust region policy optimization, in: International Conference on Machine Learning, 2015, pp. 1889–1897.
- [6] J. Peters, K. Mülling, Y. Altun, Relative entropy policy search., in: AAAI, Atlanta, 2010, pp. 1607–1612.
- [7] A. Abdolmaleki, B. Price, N. Lau, L. P. Reis, G. Neumann, Deriving and improving cma-es with information geometric trust regions, in: Proceedings of the Genetic and Evolutionary Computation Conference, ACM, 2017, pp. 657–664.
- [8] A. Abdolmaleki, R. Lioutikov, J. R. Peters, N. Lau, L. P. Reis, G. Neumann, Model-based relative entropy stochastic search, in: Advances in Neural Information Processing Systems, 2015, pp. 3537–3545.

- [9] A. Zimin, G. Neu, Online learning in episodic markovian decision processes by relative entropy policy search, in: *Advances in neural information processing systems*, 2013, pp. 1583–1591.
- [10] C. Daniel, G. Neumann, J. R. Peters, Hierarchical relative entropy policy search, in: *International Conference on Artificial Intelligence and Statistics*, 2012, pp. 273–281.
- [11] C. M. Bishop, *Pattern Recognition and Machine Learning*, Springer, 2006.
- [12] S. Nowozin, B. Cseke, R. Tomioka, f-gan: Training generative neural samplers using variational divergence minimization, in: *Advances in Neural Information Processing Systems*, 2016, pp. 271–279.
- [13] S.-I. Amari, α -divergence is unique, belonging to both f -divergence and bregman divergence classes, *IEEE Transactions on Information Theory* 55 (11) (2009) 4925–4931.
- [14] S. Bubeck, et al., Convex optimization: Algorithms and complexity, *Foundations and Trends® in Machine Learning* 8 (3-4) (2015) 231–357.
- [15] W. Krichene, A. Bayen, P. L. Bartlett, Accelerated mirror descent in continuous and discrete time, in: *Advances in Neural Information Processing Systems*, 2015, pp. 2845–2853.
- [16] E. Theodorou, J. Buchli, S. Schaal, A generalized path integral control approach to reinforcement learning, *Journal of Machine Learning Research* 11 (Nov) (2010) 3137–3181.
- [17] E. Theodorou, J. Buchli, S. Schaal, Reinforcement learning of motor skills in high dimensions: A path integral approach, in: *Robotics and Automation (ICRA)*, 2010 IEEE International Conference on, IEEE, 2010, pp. 2397–2403.
- [18] N. Hansen, A. Ostermeier, Completely derandomized self-adaptation in evolution strategies, *Evolutionary computation* 9 (2) (2001) 159–195.
- [19] J. Schulman, F. Wolski, P. Dhariwal, A. Radford, O. Klimov, Proximal policy optimization algorithms, arXiv preprint arXiv:1707.06347.
- [20] E. Theodorou, D. Krishnamurthy, E. Todorov, From information theoretic dualities to path integral and kullback-leibler control: Continuous and discrete time formulations, in: *The Sixteenth Yale Workshop on Adaptive and Learning Systems*, 2013.
- [21] F. Stulp, O. Sigaud, Policy Improvement Methods: Between Black-Box Optimization and Episodic Reinforcement Learning, 34 pages (Oct. 2012).
URL <https://hal.archives-ouvertes.fr/hal-00738463>
- [22] E. A. Theodorou, E. Todorov, Relative entropy and free energy dualities: Connections to path integral and kl control, in: *Decision and Control (CDC)*, 2012 IEEE 51st Annual Conference on, IEEE, 2012, pp. 1466–1473.
- [23] S. Mahadevan, B. Liu, Sparse q-learning with mirror descent, in: *Proceedings of the Twenty-Eighth Conference on Uncertainty in Artificial Intelligence, UAI’12*, AUAI Press, Arlington, Virginia, United States, 2012, pp. 564–573.
URL <http://dl.acm.org/citation.cfm?id=3020652.3020712>
- [24] W. H. Montgomery, S. Levine, Guided policy search via approximate mirror descent, in: *Advances in Neural Information Processing Systems*, 2016, pp. 4008–4016.
- [25] S. Levine, V. Koltun, Guided policy search, in: *Proceedings of the 30th International Conference on Machine Learning (ICML-13)*, 2013, pp. 1–9.
- [26] W. Krichene, S. Krichene, A. Bayen, Efficient bregman projections onto the simplex, in: *Decision and Control (CDC)*, 2015 IEEE 54th Annual Conference on, IEEE, 2015, pp. 3291–3298.
- [27] P. Billingsley, *Probability and measure*, John Wiley & Sons, 2008.
- [28] M. P. Deisenroth, G. Neumann, J. Peters, et al., A survey on policy search for robotics., *Foundations and Trends in Robotics* 2 (1-2) (2013) 1–142.
- [29] F. Stulp, O. Sigaud, Path integral policy improvement with covariance matrix adaptation, in: *Proceedings of the 29th International Conference on Machine Learning (ICML)*, 2012, pp. 1547–1554.
- [30] A. J. Ijspeert, J. Nakanishi, S. Schaal, Learning attractor landscapes for learning motor primitives, in: *Advances in neural information processing systems*, 2003, pp. 1547–1554.
- [31] H. Kappen, *Optimal control theory and the linear bellman equation*, Barber, D.; Cemgil, AT; Chiappa, S.(ed.), *Bayesian time series models* (2011) 363–387.
- [32] S. Shalev-Shwartz, et al., Online learning and online convex optimization, *Foundations and Trends®*

- in *Machine Learning* 4 (2) (2012) 107–194.
- [33] B. Dai, N. He, H. Dai, L. Song, Provable bayesian inference via particle mirror descent, in: *Artificial Intelligence and Statistics*, 2016, pp. 985–994.
 - [34] D. Wierstra, T. Schaul, T. Glasmachers, Y. Sun, J. Peters, J. Schmidhuber, Natural evolution strategies., *Journal of Machine Learning Research* 15 (1) (2014) 949–980.
 - [35] G. Raskutti, S. Mukherjee, The information geometry of mirror descent, arXiv preprint arXiv:1310.7780.